

# Numerical Modeling of Oil Slick Spread in the Persian Gulf

M. Soltanpour<sup>1\*</sup>, N. Wijayaratna<sup>2</sup>, Z. Hajisalimi<sup>3</sup>

<sup>1</sup> \* Civil Eng. Department, K. N. Toosi University of Technology, Tehran, Iran; [soltanpour@kntu.ac.ir](mailto:soltanpour@kntu.ac.ir).

<sup>2</sup> Faculty of Engineering, University of Ruhuna, Galle, Sri Lanka.

<sup>3</sup> Civil Eng. Department, K. N. Toosi University of Technology.

## ARTICLE INFO

### Article History:

Received: 2 January 2013

Accepted: 17 April 2013

Available online: 30 June 2013

### Keywords:

Oil slick

Persian Gulf

Numerical modeling

Trajectory

Spill

## ABSTRACT

An oil spill model coupled with a hydrodynamic model was developed to simulate the spread of oil slick in real marine conditions considering the effects of tidal currents, wind and wave. The hydrodynamic model is verified using the measurements of tidal elevations and current speeds at the Persian Gulf. Effect of various governing factors on oil slick movement, tidal currents, wind and wave, are examined. It is concluded that the wind action is the predominant factor for the spreading of oil while the overlaying waves are the second important driving force. Although the tidal currents spread the oil slick on a wider area, they have limited influences on the net transformation of slick. The performance of the model on a field data in the Persian Gulf shows that the present model is capable to predict the spread of oil in early days of the oil spill.

## 1. Introduction

Study of oil slick spreading in marine environments is important for preserving natural assets from the possible environmental damages. The prediction of the oil slick trajectory helps the managers of the coastal areas to reduce the significant and wide-ranging impacts that oil can cause in the marine environment. Although the numbers and volumes of oil spilled from tanker accidents has generally decreased in recent years [1], the study is still crucial in the Persian Gulf considering the huge traffic of oil tankers through the area and the fragile political stability of region. Oil spills may also cause damages to seawater intakes which are particularly important in the Persian Gulf region [2].

Different numerical models have been used to simulate the transport and the fate of oil slicks in the Persian Gulf (e.g. [3], [4], [5]). Some of the investigations led to the development of a series of more sophisticated oil spill models; such GULFSLIK I to IV, that are primarily focused on predicting oil spill transport over the Persian Gulf environment. Galt et al. applied the OSSM model of the US National Oceanic and Atmospheric Agency (NOAA) to the Nowruz oil spill which occurred in 1983 in the north of the Persian Gulf [6]. Murty and El-Sabh applied the IOS-UQAR model to simulate the same spill [7]. GULFSLIK II and OILPOL were applied by Al-rabeh et al. to simulate the fate and transport of Al-Ahmadi oil spill [5]. A tide and surge forecasting model

capable of predicting conditions has been developed by Proctor et al. to provide environmental data on tides, currents and particle trajectories in the Persian Gulf [8]. An oil spill response model was applied by Spaulding et al. to predict the transport and fate of oil from the Mina Al Ahmadi spill in the northern Persian Gulf which predicts the drift, spread, evaporation, dispersion, emulsification and shoreline interaction of the spilled oil [9]. The output from the modified version of a hydrodynamic numerical model developed earlier by El-Sabh and Murty (1988) has been used by Venkatesh *et al.* to hindcast the movement and dispersion of oil slicks in the Persian Gulf during part of the period of January to March 1991 [10].

A time dependent model is presented here to simulate the track of oil spill. Tidal currents are simulated using a two dimensional depth averaged hydrodynamic model. The hydrodynamic model is used to quantify the advection of oil on the ocean surface due to wind, wave and tidal currents. Drift of oil due to spread, dispersion and mass transfer are then added with the advection component. The application of the model for an actual oil spill in the Persian Gulf is presented where the oil trajectory data from satellite images is used.

## 2. General Behaviour of Oil Slick

The transport and fate of spilled oil in water bodies are governed by variety of physical, chemical, and

biological processes that depend on the oil properties, hydrodynamics, meteorological and environmental conditions. These processes include advection, turbulent diffusion, surface spreading, evaporation, dissolution, emulsification, sedimentation and the interaction of oil slick with the shoreline. When liquid oil is spilled on the sea surface, it spreads to form an oil slick, where its movement is governed by the advection and turbulent diffusion due to current, waves and wind action. Light fractions evaporate, water soluble components dissolve in the water column, and immiscible components become emulsified and dispersed in the water column as small droplets. Thus, the composition of the oil changes from the initial time of the spill. Turbulence highly affects the formation of oil in water or water-in-oil emulsion but this usually occurs within days after the initial spill [11]. Figure 1 shows a schematic representation of the transport and weathering processes [12]. However, including all these complex processes are extremely difficult to apply in real field conditions. Considering the relatively short period of simulation, of about 20 days, the complex three-dimensional phenomena of the fate of oil can be neglected. Therefore a two-dimensional depth averaged hydrodynamic model is used for the modeling of the tidal generated currents. When an oil slick is occurred, it is transported from the point of spill mostly under the effects of winds, waves and tidal currents. Hence drift, dispersion, and mass transfer can be treated as the dominant modes of oil slick movement.

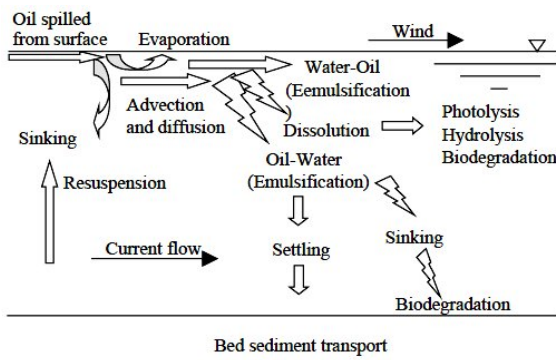


Figure 1. Transport and fate of oil slick in seas [12]

## 2.1 Drifting of oil slick

Drifting of oil due to the advection is mainly due to winds and currents. Although in some models the governing equations of the wind driven currents are solved (e.g. [13]), here the drift due to wind is estimated using the simple method proposed by Hoult [14]. He argued that the turbulent shear-stress loss at the water interface was approximately the same in the both the air and the water. Assuming the placing of oil at the air water interface would not change the shear stress, he suggested the wind driven current speed is approximately 3% of wind velocity. The drift due to tidal currents was simply taken to be tidal current

velocity. When both wind-driven currents and tidal currents are present, he suggested simply adding the two vector quantities.

The wind driven current velocity equal to 3% of wind speed has widely been used by other researchers although some believe this approximation is correct only for steady state winds [15]. They suggested taking account the coriolis effect and emphasized the importance of vertical eddy viscosity.

Reisbig *et al.* found the wind drift and wave drift mechanisms were not simply additive over all regimes of wind speed [16]. They believe the wave drift had shown to provide an augmentation to the wind drift at low wind speeds. However the waves can cause a net decrease in the coupled drift velocity at higher wind speeds.

Since the usages of empirical relationships in most of the approaches, the approximate drift of 3% of wind velocity adopted in this study looks a proper choice for simple treatment of drifting oil slick.

## 2.2 Spreading of oil slick

Formulas are available for calculating the extent of the spread of oil slicks on water as a function of time. They are based on empirical measurements of spreading rates and theoretical studies of the physical processes which accelerate or retard the spread of an oil film.

According to Fay, the oil film would pass through three stages as the time progresses [17]. He proposed three formulas for different stages. In the first stage or 'inertial spread', the gravity-inertia force dominates. As the oil film becomes thinner, the gravity force diminishes and oil slick enters to the 'viscous spread' stage. The gravity and viscous force control the spread at this stage. Finally as the oil film becomes very thin, surface tension and viscous forces counteract. Fay named this stage as the 'surface tension spread'. As the time passes further on, the viscous retardation would eventually overcome the surface tension force and the spread ceases.

Hoult showed these findings represent the similarity solutions for Navier-Stokes equations [14].

## 2.3 Mass transfer of oil slick

Oil mass removal due to weathering is very important in long term predictions of the fate of oil slick. Weathering mainly includes emulsification, chemical and biological degradation and evaporation. Since the most significant cause of oil mass removal during the first few days of spread is evaporation, it is included in the mathematical formulations in the present study.

A formula for the rate of evaporation was given by Blokner, as a function of geometry of the slick, physical properties of oil, wind speed and the time [18]. The time dependent extent of this evaporation was quantified by Sivadier and Mikolaj [19]. According to them, the oil losses most of its volatile

components in one to two hours, and then the evaporation process stops.

### 3. Hydrodynamic Model

#### 3.1. Introduction

Ocean hydrodynamics can be represented by continuity and momentum equations. Simplifications are done in the depth averaged models by eliminating the vertical axis assuming that the accelerations, velocity and eddy viscosity in the vertical direction are negligible. There are also three dimensional models which simulate the hydraulic parameter variations in different depths. These models are usually applied on limited coastal areas where better computational accuracy is required. It is difficult to calibrate these models because of the large number of unknowns.

Density and thermal-driven currents in the Persian Gulf are small except in the vicinity of the Arvand River and the Strait of Hormoz [20]. Here, the tide generated currents are simulated using a two-dimensional depth averaged hydrodynamic model. The depth averaged continuity and momentum equations can satisfactorily simulate the tidal generated currents in the Persian Gulf considering the shallow depth of the gulf compared to the tide wave length.

#### 3.2 Governing equations

The governing equations are the momentum equations in X and Y directions and continuity equation

$$\frac{\partial u}{\partial t} + u \frac{\partial u}{\partial x} + v \frac{\partial u}{\partial y} + g \frac{\partial \eta}{\partial x} - f_c v + f u \frac{(u^2 + v^2)^{1/2}}{(\eta - z)} = 0 \quad (1)$$

$$\frac{\partial v}{\partial t} + u \frac{\partial v}{\partial x} + v \frac{\partial v}{\partial y} + g \frac{\partial \eta}{\partial y} + f_c u + f v \frac{(u^2 + v^2)^{1/2}}{(\eta - z)} = 0 \quad (2)$$

$$\frac{\partial \eta}{\partial t} + \frac{\partial}{\partial x} [(\eta - z)u] + \frac{\partial}{\partial y} [(\eta - z)v] = 0 \quad (3)$$

where  $u$  and  $v$  represent velocity in X and Y directions, respectively. Parameters  $f$ ,  $f_c$  and  $\eta$  are the friction factor, the Coriolis acceleration and water surface elevation, respectively.

Effective stress terms are not included in the above momentum equations. However, the action of effective stresses is simulated by a velocity averaging technique which employs an averaging factor  $\alpha$  to vary the magnitude of the effect. Numerical eddy diffusivity  $\varepsilon$  is used to represent the effective stresses [18].

$$\frac{1}{\rho h} \left[ \frac{\partial}{\partial x} \left( h D_{xx} \frac{\partial u}{\partial x} \right) \right] + \frac{1}{\rho h} \left[ \frac{\partial}{\partial y} \left( h D_{xy} \frac{\partial u}{\partial y} \right) \right] = \varepsilon \left( \frac{\partial^2 u}{\partial x^2} + \frac{\partial^2 u}{\partial y^2} \right) \quad (4)$$

$$\frac{1}{\rho h} \left[ \frac{\partial}{\partial x} \left( h D_{xy} \frac{\partial v}{\partial x} \right) \right] + \frac{1}{\rho h} \left[ \frac{\partial}{\partial y} \left( h D_{yy} \frac{\partial v}{\partial y} \right) \right] = \varepsilon \left( \frac{\partial^2 v}{\partial x^2} + \frac{\partial^2 v}{\partial y^2} \right) \quad (5)$$

where the eddy diffusivity parameter  $\varepsilon$  is simulated through the following expression:

$$\varepsilon = \alpha (\Delta x)^2 / 2 \Delta t \quad (6)$$

The computational procedure is a multi-operational mode solution based on the division of each time step in to two-stages of a half-time step each [16]. Alternating-Direction Implicit (ADI) method is used for the computation of unknowns. The ADI method includes two explicit schemes in such a way that each stage contains an implicit scheme followed by an explicit scheme. A velocity averaging process is carried out after each step to smooth the velocity field which is dealt elsewhere. The solution procedure can be summarized as shown in the following two stages.

First stage:

1- Implicit solution of  $u^{n+1/2}$  and  $\eta^{n+1/2}$  using the continuity and X-momentum equations.

2- Explicit solution of  $v^{n+1/2}$  using the Y-momentum equation.

3- Spatial smoothing of  $u^{n+1/2}$  and  $v^{n+1/2}$  using a velocity averaging scheme.

Second stage:

1- Implicit solution of  $v^{n+1}$  and  $\eta^{n+1}$  using the continuity and Y-momentum equations.

2- Explicit solution of  $u^{n+1}$  using the X-momentum equation.

3- Spatial smoothing of  $u^{n+1}$  and  $v^{n+1}$  using a velocity averaging scheme.

#### 3.3. Finite difference equations

Spatial derivatives are expressed in terms of central differences, whereas temporal derivatives are represented by backward difference scheme. Figure 2 shows the space averaging scheme used in formulation of finite difference equations.

#### 3.4. Boundary conditions

Closed and open boundaries are specified in the model. The velocity perpendicular to a closed boundary is set to zero and there is no mass flux perpendicular to this boundary. The water surface elevations or velocities should be defined at the open boundaries. They can be extracted from a coarse grid model or generated using tidal constituents at the open

boundary.

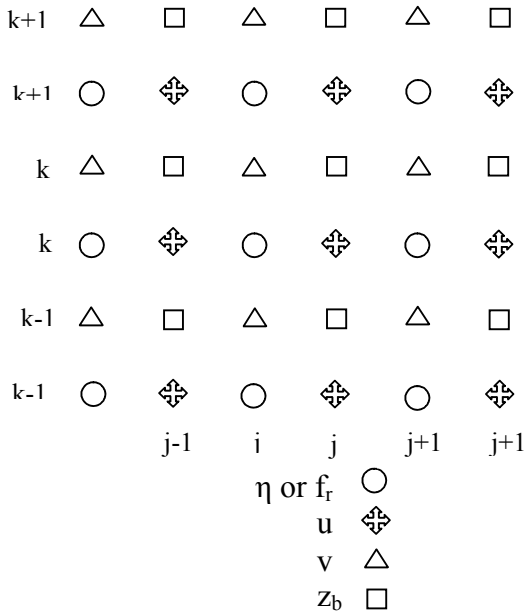


Figure 2. Finite difference grid arrangements in ADI scheme

Considering that the adopted centered finite difference method requires the information that lies outside of the boundary, a relocation technique is employed, by which exterior values are set to be equal to those interior values adjacent to the boundaries [22,23].

The input geometry and bathymetry data are introduced using two matrices defining wet and dry cells where bathymetry data is relevant to wet cells. Locations for the cells on the open boundary are introduced in the first matrix.

## 4. Modeling of Oil Spill Trajectory

### 4.1 Advection of oil slick

Advection of oil slick is considered as a superposition of the drifts due to the wind, wave, tidal currents and fresh water flow driven currents. Thus, all the current components are vectorially added to find the net drift of oil slick. Drifts due to wind and wave are considered to be in the wind direction. The effects of fresh water flow can be included in the hydrodynamic model, hence not necessary to treat it separately.

Wind induced surface current is approximately expressed as %3 of wind speed measured 10 m above still water level.

Wave induced drift is also taken to be in the wind direction. The modified Stoke's formula by Vongvisessomjai *et al.* is employed for the computation of the drift due to waves [24]:

$$U = \pi^2 \left( \frac{H}{L} \right)^2 c + 0.445 \left( \frac{H}{L} \right) c \quad (7)$$

where  $H$ ,  $L$  and  $c$  are wave height, wave length and wave celerity, respectively.

### 4.2. Spreading of oil slick

Four basic forces are acting on oil elements floating on water namely, gravity, inertia, surface tension and viscous forces. Spreading of oil slick is treated in three different stages depending on which phenomenon is dominating in the spreading process [22]:

(i) Inertial spread

$$R(t) = 1.14((\rho_w - \rho_o) / \rho_w * g V t^2)^{1/4} \quad (8)$$

(ii) Viscous spread

$$R(t) = 1.45((\rho_w - \rho_o) / (\rho_w v^{1/2}) * (V^2 t^{3/2}))^{1/6} \quad (9)$$

(iii) Surface tension spread

$$R(t) = 2.30(\sigma^2 t^3 / \rho_w^2 v)^{1/4} \quad (10)$$

where

$t$  = time since initiation of spread

$R(t)$  = radius of oil slick at time  $t$

$V$  = total spill volume

$g$  = acceleration of gravity

$\rho_w$  = density of watery

$\rho_o$  = density of oil

$v$  = kinematic viscosity of water

$\sigma$  = surface tension

The governing equation is chosen based on the thickness of oil film. Following Wang and Hwang, the thickness of each of spread criteria is limited assuming a uniform thickness distributing all over the slick area [26].

### 4.3 Oil mass removal due to weathering and evaporation

The rate of evaporation is very high in the first few hours of spill. It diminishes as all the volatile components of the oil removed from the slick. Blokker suggested a formula for the rate of evaporation as a function of slick area, wind speed, time, temperature and the physical properties of oil [18].

## 5. Data from Actual Spillage

Huge amount of oil was released into the Persian Gulf during the period of the invasion of Iraqi forces to Kuwait. The Environmental Protection Council (EPC) of Kuwait reported that the crude oil spill, started on January 19, 1991 from tankers and oil terminals, were up to 10 million barrels (420 million gallons). Figure 3 shows the sources of oil spill. Most of the oil was released at or near Mina Al-Ahmadi in southern Kuwait with a volume as large as 6 million barrels [5].

The actual spillage in the Persian Gulf was later studied to assess the observed environmental damages in Iran. NOAA-AVHRR images from NOAA-9, 10, 11 and 12 satellites during 1991 were used for tracking the oil spills and smoke plumes of Kuwait's oil fires to the coast and territory of Iran [27].

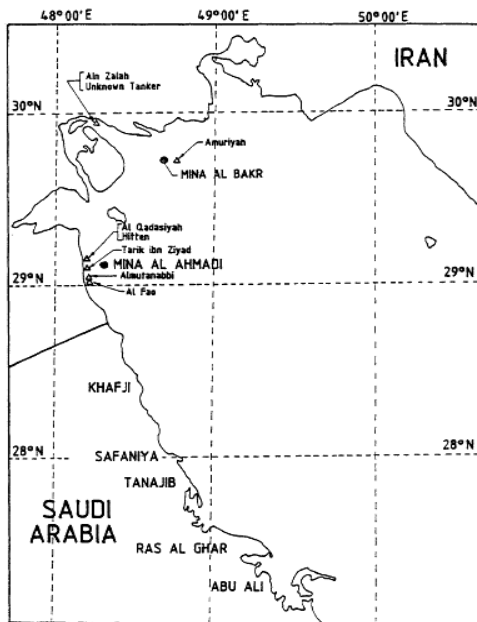


Figure 3. Main sources of spilled oil to the Persian Gulf [5]

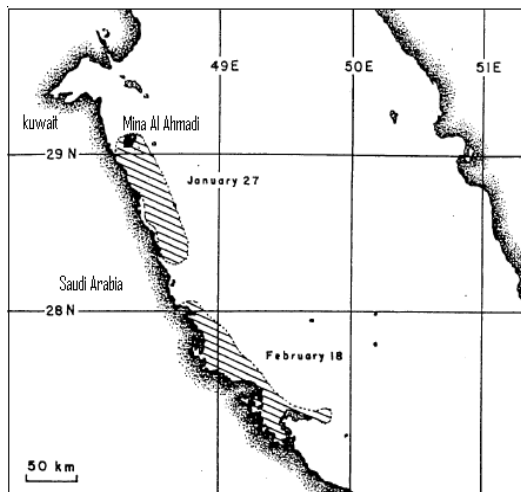


Figure 4. sketch of the Mina Al Ahmadi spill on 27 January 1991 based on a pentagon press briefing from general Schwarzkopf and overflight observations of the spill on the morning of 19 February 1991 provided by the International Interagency Oil Spill Assessment Team [9]

In the forward inspection approach, slick appeared to extend over  $144 \text{ km}^2$  on 29th of January 1991. When first observed on 24<sup>th</sup> of January 1991, the slick had a surface area of about  $200 \text{ km}^2$ . This decreased slowly to about  $155 \text{ km}^2$  by 4<sup>th</sup> of February and then much more rapidly to only  $20 \text{ km}^2$  on 12<sup>th</sup>, the last date on which it was observed on the AVHRR images. The slick moved a total distance of 173 km between 24<sup>th</sup> of January and 12<sup>th</sup> of February, or just over 9 km per day in a generally southerly direction. However, the actual daily movement varied from less than 5 km to more than 20 km.

Figure 4 shows the observations of the surface oil based on an analysis of aerial overflight data for 27<sup>th</sup> of January and 18<sup>th</sup> of February, 1991. The sketch of January 27<sup>th</sup> is from the Pentagon press briefing that day. The information of February 18<sup>th</sup> was obtained

from the International Interagency Oil Spill Assessment Team.

## 6. Modeling of Oil Spillage

### 6.1. Hydrodynamic model

The developed 2D hydrodynamic model has been already applied and calibrated for the gulf of Thailand [27]. Calibration was carried out for both water surface elevations and tidal currents showing a good agreement.

The hydrodynamic model is applied here to simulate the tidal currents in the Persian Gulf.

The water levels generated using the tidal constituents at Hengam Island is used as the open boundary condition. The location of Hengam at the Strait of Hormoz is suitable to represent the water level entering into the Persian Gulf.

Admiralty method was employed using four main tidal constituents ( $M_2$ ,  $S_2$ ,  $K_1$  and  $O_1$ ) provided by United Kingdom Hydrographic Office (UKHO) or the Admiralty Tide Tables to simulate the water level at Hengam. This method constitutes a simplified and expeditious way for the prediction and analysis of tides when the harmonic constituents are obtained from the Admiralty data.

The grid spacing in both horizontal directions and time steps are assumed as 3 km and 90 seconds, respectively. The characteristic limit  $\beta$  in Courant instability criteria is equal to 0.881 considering the maximum depth of 88 m. The model was run for 15 days between 1<sup>st</sup> and 15<sup>th</sup> of January 2009 including both neap and spring tides and the water level elevations at different locations of the Persian Gulf were simulated. Figures 5, 6, 7 and 8 present the comparisons between the calculated and simulated water levels at Kangan, Lavan Island, Khark Island and Al-Ahmadi, respectively. A relatively good agreement is observed at all locations.

Two simulated snapshots of the tidal current patterns in the Persian Gulf during ebb and flood are also presented in figures 9 and 10, respectively.

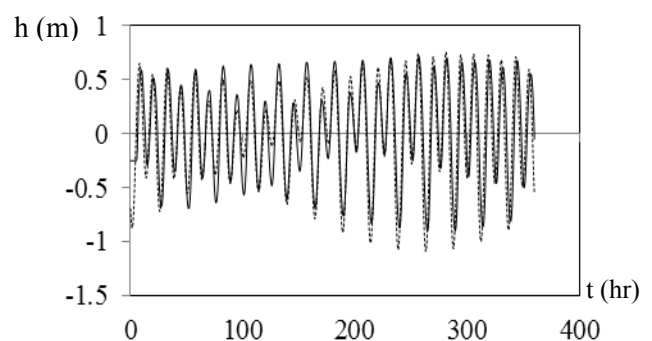


Figure 5. Comparison between simulated (dashed line) and measured (solid line) water levels at Kangan (1<sup>st</sup> to 15<sup>th</sup> of January 2009)



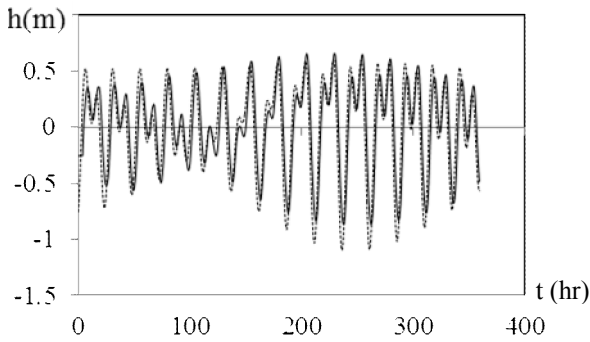


Figure 6. Comparison between simulated (dashed line) and measured (solid line) water levels at Lavan Island (1<sup>st</sup> to 15<sup>th</sup> of January 1991)

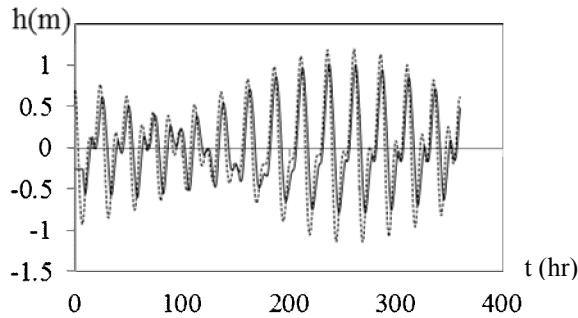


Figure 7. Comparison between simulated (dashed line) and measured (solid line) water levels at Khark Island (1<sup>st</sup> to 15<sup>th</sup> of January 1991)

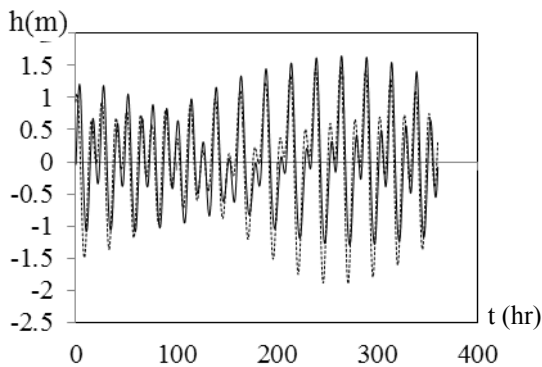


Figure 8. Comparison between simulated (dashed line) and measured (solid line) water levels at Al-Ahmadi (1<sup>st</sup> to 15<sup>th</sup> of January 1991)

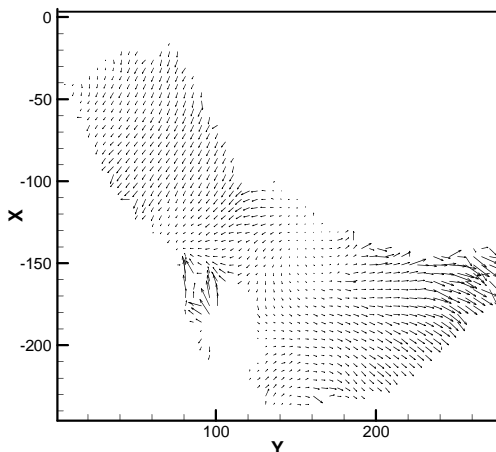


Figure 9. A snapshot of tidal current vectors during ebb tide

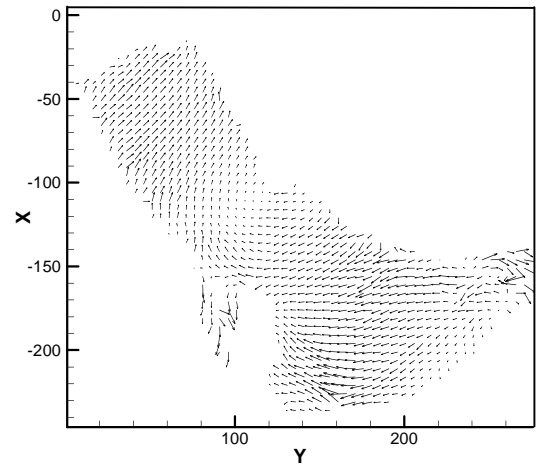


Figure 10. A snapshot of tidal current vectors during flood tide

## 6.2. Wind and Wave Data

There is no wind measurement carried out at the location of oil spill.

The wind and wave data during oil slick was adopted from the outputs of a new hindcast model at Ports and Maritime organization (PMO) for the Persian Gulf [29]. Using the synoptic station wind data around the Persian Gulf, the hindcast offers the spatial varying wind and wave data from January 1984 to end of May 2009.

The wind speed and direction and wave characteristics at study area from Jan 24<sup>th</sup> to Feb 12<sup>th</sup>, 1991 were fed into the model. Figure 11 shows the wind rose at Al-Ahmadi during the oil slick.

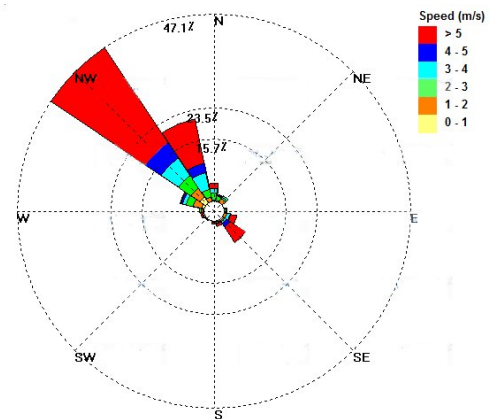


Figure 11. Wind rose at Al-Ahmadi from Jan 24<sup>th</sup> to Feb 12<sup>th</sup>, 1991

## 6.3 Simulation of Actual Spillage

The oil trajectory model is run for 26 days from Jan 24<sup>th</sup> to Feb 18<sup>th</sup>, 1991 where the tidal currents are derived from the outputs of hydrodynamic model. The effects of wind, wave and tidal currents are taken into account. An oil spill size of 240 million gallons was assumed at or near Al-Ahmadi terminal. The effects of wind, wave and tidal currents are taken into account. The outputs of the model, extracted on 27<sup>th</sup> January, 12<sup>th</sup> February and 18<sup>th</sup> February, are compared with the observations of oil slick.

Figure 12 shows the predicted location of oil slick on 27<sup>th</sup> of January, 1991. Similarly, the model results on 12<sup>th</sup> and 18<sup>th</sup> of February are presented by figures 13 and 14, respectively. The arrows reveal the Northwest to Southeast movement of oil slick. The presented results of figures 12 and 14 are comparable with the actual observed data of figure 4. The predicted location of oil slick at 12<sup>th</sup> of February also agrees with the reported track of oil slick, i.e. 173 km toward Southeast direction, based on satellite images [27]. The accumulative distribution of oil slick during total simulation period (26 days) of spillage has been presented in figure 15.

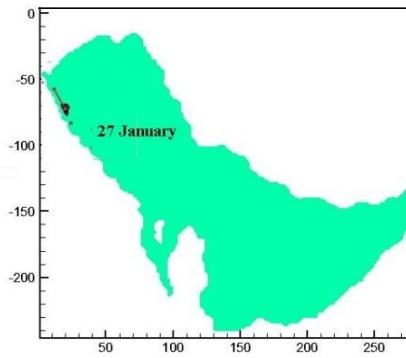


Figure 12. Predicted location of oil slick from Jan 24th to 27th, 1991(4 days)

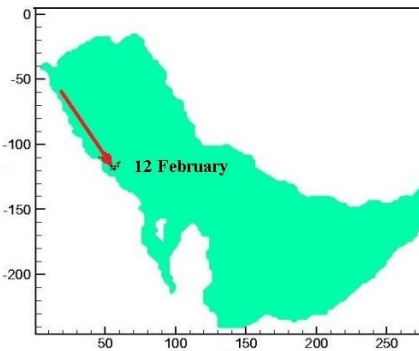


Figure 13. Predicted location of oil slick from Jan 24th to Feb 12th, 1991(20 days)

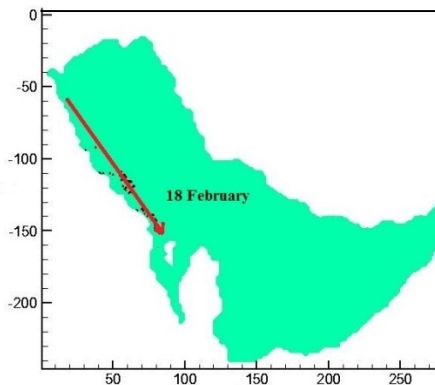


Figure 14. Predicted location of oil slick from Jan 24th to Feb 18th, 1991(26 days)

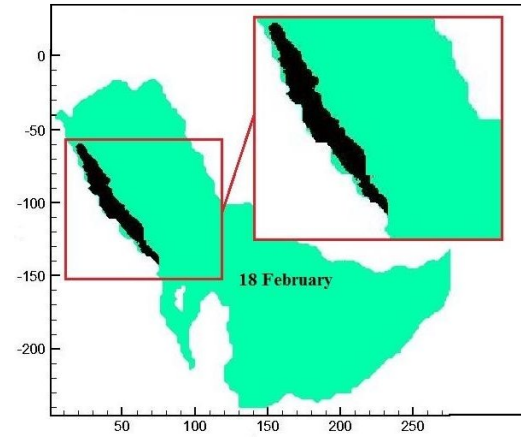


Figure 15. Accumulative distribution of oil slick from Jan 24th to Feb 18th, 1991 (all time steps)

#### 6.4. Sensitivity Analysis

The weights of the major governing factors on the driving of the oil slick are different. Using the developed oil trajectory model, the contribution of each factor can be examined.

Ignoring the wind speed and wave height, the model was run for tidal currents. Figures 16 and 17 illustrate the predicted transport of Al-Ahmadi oil terminal due to tidal forcing after 20 days and the corresponding accumulative distribution in this period, respectively. It is observed that the tidal forces result in periodic movements and scattering of oil particles and they have a small contribution to the net transport.

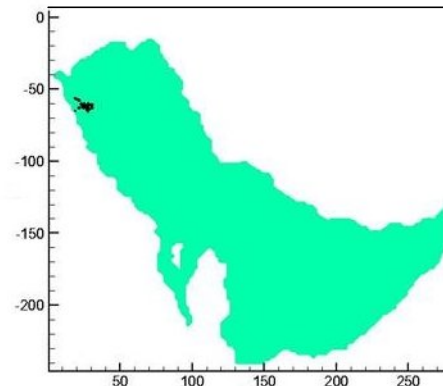


Figure 16. Predicted location of oil slick after 20 days from the start of spill due to tidal currents

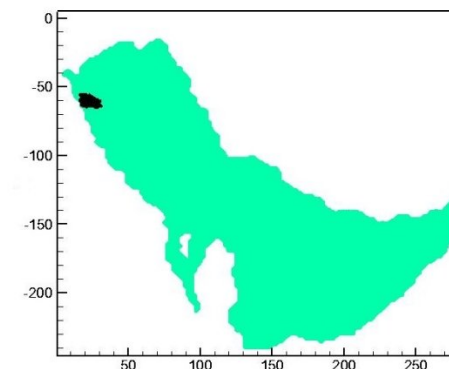


Figure 17. Accumulative distribution of oil slick from Jan 24<sup>th</sup> to Feb 12<sup>th</sup>, 1991 due to tidal currents

Figures 18 and 19 show the output results of oil spillage model under wind action. It is observed that wind-driven currents play the major role on the transport of oil slick. Similar calculations under wave action reveal that although the waves are also effective to transport oil slick, they show a much lower contribution of oil slick transport of about one fifth, compared with the transport under wind action (figures 20 and 21).

The combination of wind and wave forces results in about 95% of the oil transport. Moreover, the increase of wave height and/or wind speed will result in a higher transport of oil slick.

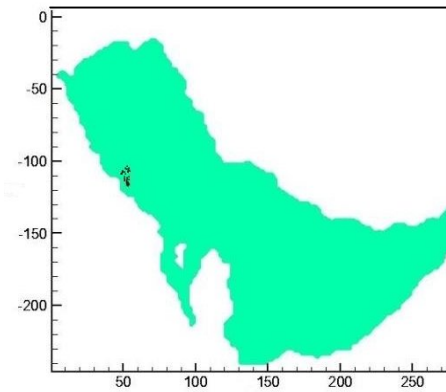


Figure 18. Predicted location of oil slick after 20 days from the start of spill due to wind-driven currents

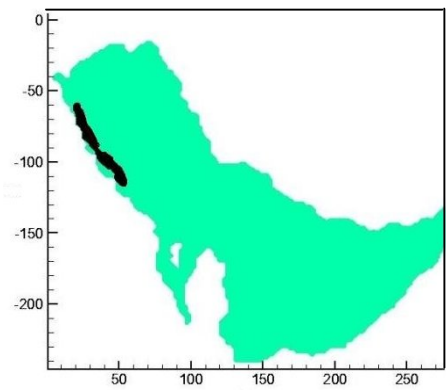


Figure 19. Accumulative distribution of oil slick from Jan 24<sup>th</sup> to Feb 12<sup>th</sup>, 1991 due to wind-driven currents

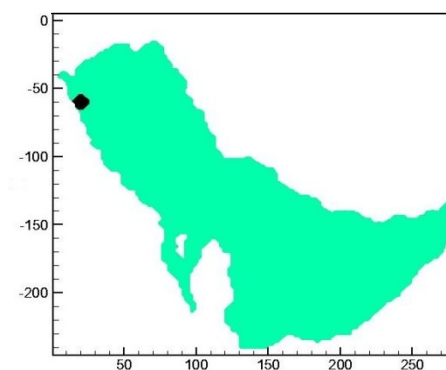


Figure 20. Predicted location of oil slick after 20 days from the start of spill due to wave-induced currents

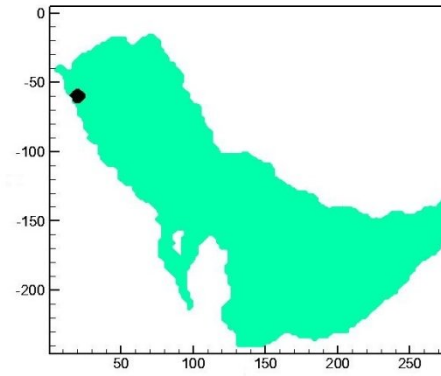


Figure 21. Accumulative distribution of oil slick from Jan 24<sup>th</sup> to Feb 12<sup>th</sup>, 1991 due to wave-induced currents

## 7. Summary and Conclusion

A numerical model was developed for the simulation of the fate of oil spills in shallow water bodies. The hydrodynamic model was calibrated for the Persian Gulf. The comparisons between the numerical results and the observed oil slick transport in the Persian Gulf shows a very good agreement for the case of oil spill that occurred at Al-Ahmadi oil terminal.

Sensitivity analysis using the developed numerical model clearly shows that tidal currents contribute very little to long-term net transport of oil spills. On the other hand, it is clear that wind-driven currents are the governing factor for the oil transport. For the case of Al-Ahmadi oil slick, the relative contributions of wind, wave and current forces are 80%, 15% and 5%, respectively.

Considering the frequency of famous Shamal winds in the Persian Gulf, the general movement of oil slicks under wind and resultant wave actions will be from northwest to southeast direction. Despite the cases where the spillage is very close to Iranian borders, the danger of oil slicks approaching Iranian borders is small. However, this fact is true for the main land and it can not be extended to the islands of the Persian Gulf. Moreover, it should be noted that although the southern winds are not frequent, they can result in a significant oil transport towards Iranian shores. Introducing the future wind field and wave forecast to the developed numerical model, it can successfully be used to predict the short term fate of oil spills in any scenario of oil spillage in the Persian Gulf.

The developed oil spill trajectory model can be improved to simulate continuous spills. However, the Fay's spreading criteria should be changed since it is valid only for the lumped spills. Long term weathering processes have to be included for long term simulations too.

## 8. Acknowledgements

The authors are grateful to Dr. S. Abbas Haghshenas, former PhD student of Civil Engineering



Department at K. N. Toosi University of Technology, for his valuable collaboration in this study.

## 9. References

1. Burgherr, P., (2007), *In-depth analysis of accidental oil spills from tankers in the context of global spill trends from all sources*, Journal of Hazardous Materials, Vol. 140 (1–2), p. 245-256.
2. Mohamed, K.A., (2007), *Minimize the negative impact of oil contamination on Abu Dhabi power and desalination plants*, Desalination Vol. 204 (1–3), p. 113-120.
3. Lehr, W. and Cekirge, H., (1979), *GULFSLICK I, a Computer Simulation of Oil Spill Trajectories in the Arabian Gulf*, Research Institute, KFUPM, Report No. 25, Saudi Arabia.
4. Lehr, W., Beenen M. S. and Cekirge, H., (1981), *Simulated oil spills at two offshore fields in the Arabian Gulf*, Marine Pollution Bulletin, 12, p. 371-374.
5. Al-rabeh, A. H., Cekirge, H. M. and Gunay, N., (1992), *Modeling the fate and transport of Al-Ahmadi oil, Water, Air, and Soil Pollution*, Vol. 65, p. 257-279.
6. Galt, J. A., Payton, D. L., Torgrimson, G. M., and Watabayashi, G., (1984), *Trajectory Analysis for the Nowruz Oil Spill*, in M. I. El-Sabh (ed.), *Oceanographic Modelling of the Kuwait Action Plan*, UNESCO Reports in Marine Sciences, No. 28, 55 p.
7. Murty, T. and El-Sabh, M. I., (1985), *Modelling the movement of oil slicks in the inner gulf of the kuwait action plan region during stormy periods: Application to the Nowruz Oil Spill*, UNEP Regional Seas Reports and studies No. 70, 279 p.
8. Proctor R., Flather R.A. and Elliott A.J., *Modelling tides and surface drift in the Arabian Gulf - application to the Gulf oil spill*, Continental Shelf Research, vol.14 (1994), p.531-545.
9. Spaulding M.L., Anderson E.L., Isaji T. and Howlett E., *Simulation of the oil trajectory and fate in the Arabian Gulf from the Mina Al Ahmadi spill*, Marine Environmental Research, vol.36 (1993), p.79-115.
10. Venkatesh S. and Murty T.S., *Numerical simulation of the movement of the 1991 oil spills in the Arabian Gulf*, Water, Air, and Soil Pollution, vol. 74 (1994), p.211-234.
11. Wang, S. D., Shena, Y. M. and Zheng, Y. H., (2005), *Two-dimensional numerical simulation for transport and fate of oil spills in seas*, Ocean Engineering, 32, p. 1556–1571.
12. Shen, H. T., Yapa, P. D., (1988), *Oil slick transport in rivers*, J. Hydraulic Eng. Vol. 114, p. 529–543.
13. Ekman, V. M., (1905), *On the influence of the Earth's rotation on ocean currents*, Ark. Mat. Astron. Fys., Vol. 2, p. 1-53.
14. Hoult, D. P., (1972), *Oil Spreading on the Sea*, Annual Review of Fluid Mechanics, Vol. 4, p. 341-368.
15. Warner, J. L., Graham, J. W. and Dean, R. G., (1972), *Prediction of the movement of an oil spill on the surface of the water*, 4<sup>th</sup> Annual Offshore Technology Conference, p. 2227-2244.
16. Reisbig, R. L., Alofs, D. J., Shah, R. C., and Banerjee, S. K., (1973), *Measurement of Oil Spill Drift Caused by the Coupled Parallel Effects of Wind and Waves*, Memories Societe Royale des Science de Leige, 6e series, tome VI: p. 67-77.
17. Fay, J. A., (1971), *Physical processes in the spread of oil on a water surface*, Conference on prevention and control of oil spills, Sponsored by API, EPA, and US Coast Guard, p. 463-467.
18. Blokker, P. C., (1964), *Spreading and Evaluation of Petroleum Products on Water*, Proceedings of 4th International Harbor Conference, Antwerp, Belgium, p. 911-919.
19. Sivadier, O. H. and Mikolaj, P. G., (1973), *Measurement of evaporation rates from oil slicks on the open sea*, Proceeding of Prevention and Control of Oil Spills, Washington D.C.
20. Lardner, R. W. and Das, S. K. (1991), *On the computation of flows driven by density gradient, Residual currents in the Persian Gulf*, Applied Mathematical Modelling, Vol. 15, Issue 6, June, p. 282-294.
21. Kuipers, J. and Vreugdwnhil, C. B., (1973), *Calculation of two-dimensional horizontal flow*, Report on basic research, S163 Part 1, Delft Hydraulics Laboratory.
22. Ponce, V. M. and Yabusaki, S. B., (1980), *Mathematical modeling of circulation in two-dimensional plane flow*, Final report to the National Science Foundation, Civil Engineering Department, Engineering Research Center, Colorado State University, Colorado.
23. Leendertse, J. J., (1968), *Use of a computational model for two-dimensional tidal flow*, Proceedings of Coastal Engineering, Vol. 1, p. 1403-1419 .
24. Vongvisessomjai, S., Arbhahirama, A. and Fuh, Y., (1978), *A mathematical model of oil spill movement-upper Gulf of Thailand*, AIT Research Report, No. 73.
25. Fay, J. A., (1969), *The Spread of Oil Slicks on a Calm Sea, Oil and the sea*, D.P. Hault Plenum Press, New York, p. 53-67.
26. Wang, S. and Hwang, L. S., (1974), *Numerical simulation of oil slick transport in bays*, Proceedings of the 4<sup>th</sup> Coastal Engineering Conference, p. 2227-2244.
27. Jalali, N., Noroozi, A. A. and Abkar, A. A., (1998), *Tracking of oil spills and smoke plumes of Kuwait's oil well fires to the coast and territory of I.R. of Iran as a result of the 1991 Persian Gulf War*,

Soil Investigation and Watershed Management Center of I.R. of Iran, 282 p.

28. Wijayaratna, T. M. N., (1997), *Oil spill trajectory model for the gulf of Thailand*, Thesis No. WM-96-6, Asian Institute of Technology.

29. Baird and Associates / Jahad Water and Energy Research Company, (2012), Study reports of *Monitoring and Modeling Study of Some Coastal Parts of Sistan and Baluchestan and Bushehr Provinces: Persian Gulf Hindcast report*, Ports and Maritime Organization (PMO), 135 p.